Available online at www.sciencedirect.com
SCIENCE DIRECT®
Earth and Planetary Science Letters 241 (2006) 477–492
EPSL
www.elsevier.com/locate/epsl

The Late Eocene $^{187}Os/^{188}Os$ excursion: Chemostratigraphy, cosmic dust flux and the Early Oligocene glaciation

Tarun K. Dalai [a,*], Gregory E. Ravizza [a], B. Peucker-Ehrenbrink [b]

[a] Department of Geology and Geophysics, SOEST, University of Hawaii at Manoa, Honolulu, HI 96822, USA
[b] Department of Marine Chemistry and Geochemistry, Woods Hole Oceanographic Institution, Woods Hole, MA 02543, USA

Received 29 March 2005; received in revised form 13 September 2005; accepted 23 November 2005
Available online 27 December 2005
Editor: E. Boyle

Abstract

High resolution records (ca. 100 kyr) of Os isotope composition ($^{187}Os/^{188}Os$) in bulk sediments from two tropical Pacific sites (ODP Sites 1218 and 1219) capture the complete Late Eocene $^{187}Os/^{188}Os$ excursion and confirm that the Late Eocene $^{187}Os/^{188}Os$ minimum, earlier reported by Ravizza and Peucker-Ehrenbrink [Earth Planet. Sci. Lett. 210 (2003) 151–165], is a global feature. Using the astronomically tuned age models available for these sites, it is suggested that the Late Eocene $^{187}Os/^{188}Os$ minimum can be placed at 34.5 ± 0.1 Ma in the marine records. In addition, two other distinct features of the $^{187}Os/^{188}Os$ excursion that are correlatable among sections are proposed as chemostratigraphic markers which can serve as age control points with a precision of ca. ± 0.1 Myr. We propose a speculative hypothesis that higher cosmic dust flux in the Late Eocene may have contributed to global cooling and Early Oligocene glaciation (Oi-1) by supplying bio-essential trace elements to the oceans and thereby resulting in higher ocean productivity, enhanced burial of organic carbon and draw down of atmospheric CO_2. To determine if the hypothesis that enhanced cosmic dust flux in the Late Eocene was a cause for the $^{187}Os/^{188}Os$ excursion can be tested by using the paired bulk sediment and leachate Os isotope composition; $^{187}Os/^{188}Os$ were also measured in sediment leachates. Results of analyses of leachates are inconsistent between the south Atlantic and the Pacific sites, and therefore do not yield a robust test of this hypothesis. Comparison of $^{187}Os/^{188}Os$ records with high resolution benthic foraminiferal $\delta^{18}O$ records across the Eocene–Oligocene transition suggests that ^{187}Os flux to the oceans decreased during cooling and ice growth leading to the Oi-1 glaciation, whereas subsequent decay of ice-sheets and deglacial weathering drove seawater $^{187}Os/^{188}Os$ to higher values. Although the precise timing and magnitude of these changes in weathering fluxes and their effects on the marine $^{187}Os/^{188}Os$ records are obscured by recovery from the Late Eocene $^{187}Os/^{188}Os$ excursion, evidence of the global influence of glaciation on supply of Os to the ocean is robust as it has now been documented in both Pacific and Atlantic records.

Keywords: Eocene–Oligocene transition; Os isotopes; chemostratigraphy; Oi-1 glaciation; paleoceanography; climate-weathering feedback

1. Introduction

The Eocene–Oligocene transition (EOT) marks an important change in Earth's global climate regime during which the unusual warmth of the Eocene gives way to the development of an extensive Antarctic ice-sheet [1–3]. This climate shift is reflected by an abrupt in-

* Corresponding author.
E-mail address: dalai@hawaii.edu (T.K. Dalai).

0012-821X/$ - see front matter © 2005 Elsevier B.V. All rights reserved.
doi:10.1016/j.epsl.2005.11.035

crease of benthic $\delta^{18}O$ in marine records near the Eocene–Oligocene boundary (EOB), commonly recognized as the "Oi-1" glaciation event [2,3]. The EOT is also characterized by a pronounced deepening of calcite compensation depth as documented in several deep sea cores ([4], see [5] for a recent summary). Furthermore, two major meteoritic impacts and a protracted cometary shower in the Late Eocene have been documented [6–8]. The causative mechanism for the Oi-1 is widely debated. For many years this climate transition was widely believed to result from opening of the Southern Ocean Gateways [1,9]. A recent study, however, suggests that opening of the Tasmanian Gateway did not cause a decrease of sea-surface temperature [10] as believed earlier. Some of the other proposed mechanisms for Oi-1 glaciation are: threshold response to long term decline of global atmospheric CO_2 [11], extraterrestrial impacts [12,13], rapid chemical weathering of silicates and associated enhanced burial of organic carbon [14,15], evolution and expansion of grasslands which served as sinks for atmospheric CO_2, CH_4 and water vapor [16], and orbital forcing [17].

Recent studies show that change in ocean composition brought about by global events and associated change in inputs to the oceans can be tracked by marine Os isotopic ($^{187}Os/^{188}Os$) records [18–20]. Marine residence time of Os, of the order of 10 to 50 thousand years, allows perturbations over 10^4 to 10^5 years to be captured by marine $^{187}Os/^{188}Os$ records. We report here $^{187}Os/^{188}Os$ records across the EOT of two sections from the tropical Pacific (Sites 1218 and 1219, ODP Leg 199). These two sites provide continuous Eocene–Oligocene records with excellent age control [17,21]. The study of [19] on $^{187}Os/^{188}Os$ records across the EOT from three sections showed a pronounced Late Eocene $^{187}Os/^{188}Os$ minimum. The results of this study, together with those of [19] provide the most comprehensive database on the marine $^{187}Os/^{188}Os$ for any interval of geological time. The major objectives of this study are: (i) to evaluate the utility of the marine Os isotopic record across the EOT as a tool for chemostratigraphic correlation. We explore for the first time the potential of correlatable features of the Late Eocene $^{187}Os/^{188}Os$ excursion as time control points in the marine sections, using the orbitally tuned age model from Site 1218 [17,21]. (ii) To determine if the hypothesis that enhanced cosmic dust flux was the cause of the Late Eocene $^{187}Os/^{188}Os$ excursion can be tested by using paired leachate and bulk sediment Os isotope compositions from sections across the EOT. (iii) To assess the role of Oi-1 glaciation and decay of ice sheets in regulating the weathering inputs to the oceans by comparing the Early Oligocene $^{187}Os/^{188}Os$ records with high resolution benthic $\delta^{18}O$ records for the EOT sections at Site 1218 recently reported in [17]. This Pacific record is complementary to the $\delta^{18}O$ of benthic foraminifera [3] and Os isotope records from the South Atlantic DSDP Site 522 [19]. We propose a new hypothesis for the origin of Oi-1 glaciation and explore the connection between the Late Eocene $^{187}Os/^{188}Os$ excursion and the Oi-1 event.

2. Sample materials and stratigraphy

The sediments used in this study are core samples from Sites 1218 and 1219 of ODP Leg 199, which successfully collected multiple Eocene–Oligocene sections in the tropical Pacific Ocean along a latitudinal transect. Site 1218 (8°53.38′ N, 135°22.00′ W, water depth 4826 m) was drilled on a 40 Myr old crust and provides the best record across the EOB. Owing to its younger crust, it is shallower than at Site 1219 and has relatively higher carbonate accumulation. Porewater chemical profiles indicate lack of significant suboxic diagenesis throughout the section. Site 1219 (7°48.01′ N, 142°00.94′ W, water depth 5063 m), the southernmost site of Leg 199 and with a basement age of ~55 Ma, provides an analog for Site 1218 on an older and deeper crust. Porewater chemistry indicates limited influence of organic matter degradation [22]. The sediments of these sections, originally deposited under the high productivity equatorial belt, have been transported into the red clay zone of slow accumulation by northward drift of the Pacific plate throughout the Cenozoic [23]. At Site 1218, the Eocene–Oligocene transition is marked by a two step up-section shift from dark radiolarite to pale nannofossil chalk, whereas at Site 1219 the transition is sharper and is associated with an abrupt lithological change from radiolarian clays below to the nannofossil ooze above [22].

Previous Os isotopic studies from the DSDP cores [19] were afflicted by gaps in core recovery (Site 574) and termination of the Late Eocene section by oceanic basement (Site 522), thus making it impossible to capture the complete Late Eocene $^{187}Os/^{188}Os$ excursion in a single section. Complete EOT sections recovered by ODP Leg 199 overcome such problems. Perhaps the most important feature of Leg 199 Eocene–Oligocene sections is excellent magnetostratigraphy and a detailed cyclostratigraphic age model. A recent study on Site 1218 provided revised age for Eocene–Oligocene boundary based on astronomical tuned age models [17]. These authors used the lithological proxy mea-

surements of multi-sensor track (MST) of the core scanner, $\delta^{18}O$, $\delta^{13}C$ and $\%CaCO_3$ data from both the sites to generate an aligned and stacked revised composite depth scale between Sites 1218 and 1219. Results of this effort indicate that the sections recovered across the EOT at these sites are continuous. The final age model integrated information from biostratigraphy, magnetostratigraphy, lithological proxies and isotopic measurements with astronomically calculated cycles of Earth's orbit and solar insolation. This revised chronology places the Eocene–Oligocene boundary at 33.9 Myr [17]. Excellent depth correlation between sites 1218 and 1219 [21] is significant as it removes the uncertainty of temporal variations in seawater $^{187}Os/^{188}Os$ and thus provide a context to evaluate whether or not the $^{187}Os/^{188}Os$ records from two sections are a result of differences in seawater composition at two locations or reflect the offset between $^{187}Os/^{188}Os$ of seawater and bulk sediments.

3. Analytical methods

Osmium and other platinum group elements (PGE) were pre-concentrated from 3–5 g of powdered samples by NiS fire assay [24] after spiking the samples with a tracer solution enriched in ^{105}Pd, ^{190}Os, ^{191}Ir and ^{198}Pt. Osmium isotopes were analyzed using a magnetic-sector inductively coupled plasma mass spectrometer (ELEMENT 2) after slightly modifying the procedure of [25]. Briefly, the modifications include the use of an additional argon gas flow in the sample inlet system and of a cyclonic spray chamber. Analysis of Os isotopes by sparging of OsO_4 vapor from the sample solution has been shown to be rapid and suitable for generating high resolution marine $^{187}Os/^{188}Os$ and PGE records [18–20] as the natural dynamic range in $^{187}Os/^{188}Os$ far exceeds the analytical precision (usually 1–2%). PGE of the bulk sediments were analyzed by isotope dilution ICPMS in aliquots of same sample solutions that were used for analysis of Os isotopes. Repeated analysis of 100 pg aliquots of an in-house Os standard during the course of this study yielded an average $^{187}Os/^{188}Os$ of 0.1096 ± 0.0039 (2 S.D., $n=36$). Bulk concentrations of Os and $^{187}Os/^{188}Os$ were measured in 60 samples. Of these 60 samples 15 were processed and measured in duplicate. The average differences in $^{187}Os/^{188}Os$ and Os concentration between duplicate analyses were ca. 1% (range: 0% to 6%) and ca. 5% (range: 0% to 20%), respectively. Analyses of seven procedural fusion blanks yielded 0.32 ± 0.09 pg/g Os with $^{187}Os/^{188}Os$ of 0.79 ± 0.21 (both 2 S.D.). The blank corrections for the total measured Os amounted to a maximum of 2.4% and averaged at 1%.

Osmium isotopes were also analyzed in the sediment leachates of sediments from Sites 522, 1218 and 1219 by directly sparging the leached solutions after treating the sample powders with 0.3 vol.% H_2O_2 in a dilute sulfuric acid medium. Earlier experiments have shown that a 6 vol.% H_2O_2 solution leaches a certain amount of non-hydrogenous Os [26]. Peucker-Ehrenbrink et al. [27] observed that leaching of sediments from the Cretaceous–Tertiary boundary with 0.33 vol.% H_2O_2 yielded very low Os concentration and more radiogenic $^{187}Os/^{188}Os$ compared to a 0.64 vol.% H_2O_2 leaching solution, presumably due to leaching of unradiogenic Os from cosmic material in the stronger leach. In light of these studies and in order to minimize leaching of non hydrogenous Os from sediments we leached the sediments with 0.3 vol.% H_2O_2. The dilute sulfuric acid used as the leaching solution was purged overnight in presence of H_2O_2 to reduce the procedural Os blank in the leachates. For some samples, leachates were spiked with an enriched ^{190}Os spike after separation from the residual sediment, a few drops of concentrated H_2O_2 (30 vol.%) were added to the spike–leachate mixture and allowed to sit overnight for spike-sample equilibration before sparging. The purpose of addition of H_2O_2 was to ensure rapid equilibration of spike-sample Os. Continuous in-run monitoring showed no unexpected variation in $^{190}Os/^{188}Os$, suggestive of spike-sample equilibration. Agreement of Os concentrations and $^{187}Os/^{188}Os$ in the leachates between replicates within ca. 5% provides additional support to this inference. Analysis of unspiked leaching solution showed that count rates of ^{190}Os signal were not statistically different than the count rates obtained by sparging the sub-boiling quartz distilled water that was used for sample processing. This suggests that Os blank associated with the leaching procedure was not high enough to influence the $^{187}Os/^{188}Os$ and Os concentrations of leachates, and that attempt at determining the Os blank in the leach would not yield statistically meaningful results. Average difference of $^{187}Os/^{188}Os$ between replicate analyses of leachates is ca. 5% that is higher compared to the bulk analysis. This could be due to sample heterogeneity and/or variable magnitude of leaching of Os from lithogenic/cosmic phases.

4. Results and discussions

Results of Os concentrations and $^{187}Os/^{188}Os$ of bulk sediment analyses are presented in Table 1 and data for the leachates in Table 2. PGE concentrations of

Table 1
Os concentration and $^{187}Os/^{188}Os$ of bulk sediment samples

Sample	Depth (rmcd)	Age (Ma)	$^{187}Os/^{188}Os$	$\pm 2\sigma$	Os (pg/g)
ODP 1218A					
1218 23X 1W 120-122	230.31	32.82	0.544	0.010	67
1218 23X 2W 140-142	231.65	32.94	0.520	0.002	82
1218 23X 3W 90-92	232.65	33.04	0.546	0.009	77
1218 23X 4W 140-142	234.65	33.26	0.496	0.002	103
1218 23X 5W 90-92	235.65	33.35	0.482	0.002	75
1218 23X 6W 50-55	236.77	33.45	0.471	0.002	44
1218 23X 6W 140-142	237.65	33.51	0.466	0.003	105
1218 23X 6W 140-142 Rep	237.65	33.51	0.437	0.002	114
1218 24X 1W 3-8	240.12	33.69	0.433	0.003	50
1218 24X 1W 60-62	240.80	33.74	0.446	0.003	108
1218 24X 1W 60-62 Rep	240.80	33.74	0.442	0.003	103
1218 24X 1W 90-95	241.17	33.78	0.430	0.003	40
1218 24X 2W 30-32	241.58	33.84	0.426	0.003	93
1218 24X 2W 60-65	241.90	33.87	0.399	0.002	36
1218 24X 2W 90-92	242.15	33.90	0.401	0.006	88
1218 24X 2W 140-145	242.62	33.96	0.364	0.005	73
1218 24X 3W 47-52	243.01	34.00	0.348	0.005	54
1218 24X 3W 120-122	243.61	34.12	0.355	0.003	98
1218 24X 3W 120-122 Rep	243.61	34.12	0.353	0.002	100
1218 24X 4W 10-12	243.95	34.21	0.322	0.002	154
1218 24X 4W 40-42	244.20	34.28	0.302	0.002	155
1218 24X 4W 100-102	244.72	34.42	0.276	0.001	141
1218 24X 5W 10-12	245.26	34.56	0.329	0.006	101
1218 24X 5W 40-42	245.53	34.65	0.288	0.001	135
1218 24X 5W 70-72	245.80	34.74	0.312	0.002	104
1218 24X 5W 100-102	246.04	34.83	0.338	0.001	102
1218 24X 6W 70-72	247.01	35.13	0.465	0.015	57
1218 24X 6W 100-102	247.25	35.19	0.481	0.004	51
1218 24X 7W 6-8	247.76	35.30	0.537	0.007	43
1218 24X 7W 80-82	248.40	35.41	0.522	0.010	47
1218 25X 1W 6-8	250.95	36.00	0.537	0.011	84
ODP 1219A					
1219 16H 3W 140-142	164.96	32.74	0.550	0.002	90
1219 16H 3W 140-142 Rep	164.96	32.74	0.550	0.003	89
1219 16H 5W 140-142	168.01	32.99	0.527	0.008	90
1219 16H 6W 5-9	168.17	33.01	0.525	0.007	56
1219 16H 6W 5-9 Rep	168.17	33.01	0.529	0.003	55
1219 16H 6W 35-37	168.46	33.02	0.512	0.002	55
1219 16H 6W 125-129	169.37	33.12	0.520	0.016	50
1219 16H 6W 125-129 Rep	169.37	33.12	0.505	0.007	52
1219 16H 7W 5-9	169.67	33.15	0.521	0.013	50
1219 16H 7W 5-9 Rep	169.67	33.15	0.530	0.022	51
1219 16H 7W 35-39	169.97	33.17	0.514	0.007	67
1219 16H 7W 35-39 Rep	169.97	33.17	0.514	0.003	71
1219 17H 1W 65-69	171.66	33.50	0.495	0.003	39
1219 17H 2W 30-39	172.84	33.62	0.480	0.002	34
1219 17H 2W 95-99	173.46	33.72	0.479	0.009	45
1219 17H 3W 5-9	173.58	33.72	0.469	0.002	55
1219 17H 3W 65-69	174.18	33.75	0.450	0.003	45
1219 17H 4W 95-99	175.32	33.90	0.411	0.002	43
1219 17H 4W 125-129	175.62	33.97	0.443	0.010	175
1219 17H 5W 65-69	176.52	34.17	0.391	0.002	46
1219 17H 5W 95-99	176.82	34.23	0.391	0.009	376
1219 17H 5W 135-139	177.22	34.32	0.335	0.001	99
1219 17H 6W 5-9	177.43	34.37	0.337	0.005	102
1219 17H 6W 5-9 Rep	177.43	34.37	0.331	0.002	104

Table 1 (*continued*)

Sample	Depth (rmcd)	Age (Ma)	$^{187}Os/^{188}Os$	$\pm 2\sigma$	Os (pg/g)
1219 17H 6W 35-39	177.73	34.44	0.326	0.003	246
1219 17H 6W 35-39 Rep	177.73	34.44	0.329	0.001	299
1219 17H 6W 65-69	178.03	34.50	0.335	0.001	93
1219 17H 6W 65-69 Rep	178.03	34.50	0.333	0.002	95
1219 17H 6W 95-99	178.33	34.57	0.318	0.004	196
1219 17H 6W 95-99 Rep	178.33	34.57	0.317	0.003	225
1219 17H 6W 125-129	178.63	34.66	0.335	0.002	102
1219 17H 6W 125-129 Rep	178.63	34.66	0.336	0.001	110
1219 17H 7W 0-4	178.88	34.75	0.368	0.002	150
1219 17H 7W 35-39	179.23	34.89	0.375	0.004	82
1219 17H 7W 3539 Rep	179.23	34.89	0.376	0.003	82
1219 17H 7W 9599	179.83	35.09	0.432	0.007	72
1219 17H 7W 95-99 Rep	179.83	35.09	0.425	0.005	72
1219 17H 7W 125-129(1)	180.12	35.17	0.465	0.001	144
1219 17H 7W 125-129(2)	180.12	35.17	0.452	0.002	94
1219 18H 1W 6-10	181.57	35.40	0.488	0.002	87
1219 18H 1W 35-39	181.86	35.44	0.366	0.005	105
1219 18H 1W 65-69	182.16	35.48	0.475	0.002	128
1219 18H 1W 125-129	182.76	35.60	0.512	0.005	84
1219 18H 3W 100-102	185.50	36.09	0.519	0.004	56

rmcd: revised meters composite depth [21]. Rep: replicate analyses. (1) and (2) indicate splits of the same sample powdered and homogenized separately. Uncertainties of $^{187}Os/^{188}Os$ are standard errors of the means.

these samples will be reported elsewhere, but are discussed briefly later on. Bulk Os concentrations ranged from 34 to 376 pg/g and are generally higher than those reported for the Eocene–Oligocene sections from the DSDP Sites 574 and 522 [19]. $^{187}Os/^{188}Os$ of the full Leg 199 data set range from 0.276 to 0.55. The records show $^{187}Os/^{188}Os$ minimum at rmcd 244.7 (rmcd=revised meters composite depth, [21]) of Site 1218 and at rmcd 178.3 of Site 1219 (Table 1, Fig. 1). Using the astronomically tuned age model [17,21], these depths translate to 34.4–34.6 Ma (the Late Eocene period). The $^{187}Os/^{188}Os$ minima are associated with elevated Os concentrations at both sites. This $^{187}Os/^{188}Os$ minimum was first observed in the red clays from the North Pacific core LL44-GPC3 [26,28]. Ravizza and Peucker-Ehrenbrink [19] showed that this $^{187}Os/^{188}Os$ minimum occurred in the Late Eocene and not at the EOB, an observation corroborated by the results of this study. Results plotted in Fig. 1 show that the complete Late Eocene $^{187}Os/^{188}Os$ excursion is captured in individual sections from both Sites 1218 and 1219. $^{187}Os/^{188}Os$ records during the Early Oligocene and before the Late Eocene $^{187}Os/^{188}Os$ minimum agree well between the two sites. However, $^{187}Os/^{188}Os$ values at Site 1218 are 5–10% lower relative to Site 1219 at and near the $^{187}Os/^{188}Os$ minimum (Fig. 1). While systematic offsets between coeval Os isotope records from different locations have been noted previously [18,19], subtle differences in seawater $^{187}Os/^{188}Os$ of different ocean basins could not be precluded as the cause of these offsets [29]. However, ODP Sites 1218 and 1219 are both located in the tropical Pacific approximately 750 km apart and differences in the $^{187}Os/^{188}Os$ of seawater between these two locations are unlikely. Variable contents of non-hydrogenous Os contained in cosmic dust and terrigenous matter, and different Os isotopic composition of terrigenous matter can all contribute to the observed difference in the magnitude of the Late Eocene $^{187}Os/^{188}Os$ minimum at these two sites. One sample (1219 18H 1W 35–39) plots off the Late Eocene Os isotope record with $^{187}Os/^{188}Os$ which is more than 0.1 unit less compared to the samples above and below it. High PGE abundances with near chondritic Pt/Ir for this sample indicate that low $^{187}Os/^{188}Os$ of this sample may have been a result of one of the Late Eocene extraterrestrial impacts [6,7].

4.1. The Late Eocene $^{187}Os/^{188}Os$ excursion: its chemostratigraphic significance

One of the important attributes of the $^{187}Os/^{188}Os$ data obtained in this study is that each of the two investigated sections individually captures the complete $^{187}Os/^{188}Os$ excursion which was documented only in the composite records of [19]. In the following we discuss the utility of Site 1218 records as a reference section for stratigraphic correlation using Os isotopes.

Table 2
Os concentration and $^{187}Os/^{188}Os$ of sediment leachates

Sample	Depth*	Age (Ma)	$^{187}Os/^{188}Os$	$\pm 2\sigma$	Os (pg/g)
ODP 1218A					
1218 23X 3W 90-92	232.65	33.04	0.537	0.013	ns
1218 23X 3W 90-92 Rep	232.65	33.04	0.503	0.008	ns
1218 23X 4W 140-142	234.65	33.26	0.470	0.013	6.5
1218 23X 4W 140-142 Rep	234.65	33.26	0.495	0.015	ns
1218 24X 1W 3-8	240.12	33.69	0.442	0.013	ns
1218 24X 1W 3-8 Rep	240.12	33.69	0.462	0.006	ns
1218 24X 1W 90-95	241.17	33.78	0.466	0.007	ns
1218 24X 3W 47-52	243.01	34.00	0.481	0.010	ns
1218 24X 4W 40-42	244.20	34.28	0.395	0.022	1.1
1218 24X 5W 40-42	245.53	34.65	0.398	0.011	ns
1218 24X 5W 70-72	245.80	34.74	0.419	0.005	ns
1218 24X 6W 100-102	247.25	35.19	0.537	0.013	ns
1218 24X 7W 6-8	247.76	35.30	0.532	0.010	ns
1218 24X 7W 80-82	248.40	35.41	0.499	0.010	ns
ODP 1219A					
1219 16H 6W 125-129	169.37	33.12	0.524	0.007	9.7
1219 16H 7W 35-39	169.97	33.17	0.526	0.008	10.5
1219 17H 4W 125-129	175.62	33.97	0.464	0.003	11.3
1219 17H 5W 95-99	176.82	34.23	0.435	0.006	8.9
1219 17H 6W 5-9	177.43	34.37	0.426	0.005	7.0
1219 17H 6W 35-39 Seq. 1	177.73	34.44	0.419	0.003	ns
1219 17H 6W 35-39 Seq. 2	177.73	34.44	0.413	0.004	ns
1219 17H 6W 65-69	178.03	34.50	0.427	0.004	8.2
1219 17H 6W 95-99 Seq.1	178.33	34.57	0.365	0.003	ns
1219 17H 6W 95-99 Seq.2	178.33	34.57	0.365	0.004	ns
1219 17H 6W 95-99	178.33	34.57	0.385	0.006	6.0
1219 17H 6W 125-129	178.63	34.66	0.444	0.004	8.1
1219 17H 7W 0-4	178.88	34.75	0.447	0.004	8.2
1219 17H 7W 35-39	179.23	34.89	0.437	0.003	17.0
1219 17H 7W 95-99	179.83	35.09	0.462	0.004	17.8
1219 17H 7W 95-99 Rep	179.83	35.09	0.454	0.004	18.9
1219 17H 7W 125-129(1)	180.12	35.17	0.480	0.004	7.0
1219 17H 7W 125-129(1) Rep	180.12	35.17	0.458	0.005	7.3
1219 18H 1W 125-129	182.76	35.60	0.420	0.007	6.7
1219 18H 2W 95-99	183.96	35.86	0.433	0.003	12.4
DSDP 522					
73-522-37H-1W-85-87	140.55	34.30	0.288	0.004	22.4
73-522-037-03W-22	142.92	34.53	0.239	0.005	21.3
73-522-038-01W-45	144.15	34.66	0.251	0.006	21.8
73-522-038-02W-21	145.41	34.78	0.267	0.010	17.8
73-522-038-03W-6	146.76	34.92	0.354	0.007	14.5

*Depth scales for Leg 199 samples in rmcd and for Site 522 samples in mbsf. Ages of the Site 522 samples are based on age model of [17]. Uncertainties of $^{187}Os/^{188}Os$ are standard errors of the means. Seq.: sequential leach. ns: not spiked.

Using the Os isotope record as a chemostratigraphic marker requires that age assignments be made based on specific features in the marine Os isotope record rather than on absolute $^{187}Os/^{188}Os$. This is due to the systematic difference in $^{187}Os/^{188}Os$ between age equivalent samples from Sites 1218 and 1219, particularly within the core of the Late Eocene excursion to the lowest $^{187}Os/^{188}Os$. Logging data provide a sound basis for detailed lithostratigraphic correlation between Sites 1218 and 1219. Comparison of the depth-variation of $^{187}Os/^{188}Os$ data at both sites, by plotting $^{187}Os/^{188}Os$ records of Site 1219 in the depth scales corresponding to the Site 1218-equivalent rmcd, show an excellent match for the Late Eocene $^{187}Os/^{188}Os$ excursion between these two sites (Fig. 2). There is good agreement for the magnitude and structure of the

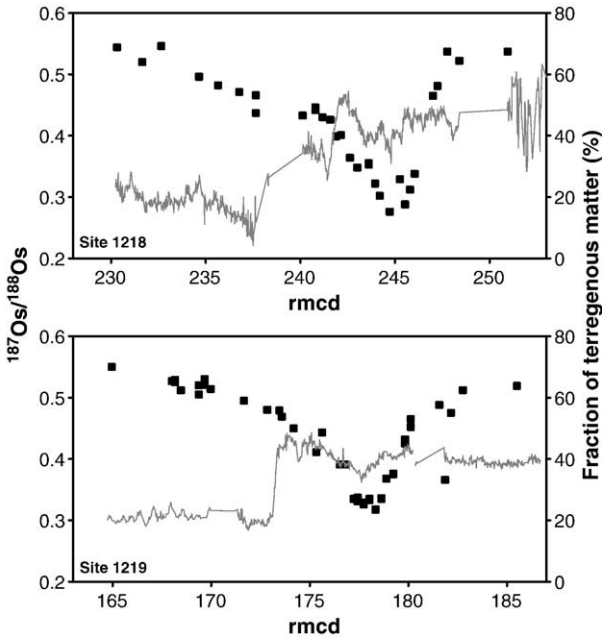

Fig. 1. Depth profile of bulk $^{187}Os/^{188}Os$ in two sections from ODP Sites 1218 and 1219 (filled squares). The two sections studied individually capture the complete Late Eocene $^{187}Os/^{188}Os$ excursion (rmcd=revised meters composite depth). Also plotted are variations in terrigenous fractions in sediments (gray lines) for the studied interval (Data from [23]). Comparison of variation in $^{187}Os/^{188}Os$ with that of fraction of terrigenous matter indicates that detrital matter exert insignificant influence on the overall $^{187}Os/^{188}Os$ records in sediments.

Late Eocene $^{187}Os/^{188}Os$ excursion across the minimum between the Site 1218 in the Pacific and Site 522 in the Atlantic (Fig. 3). Considering that these two sites are located in different ocean basins, the value of the Late Eocene $^{187}Os/^{188}Os$ minimum (~0.27–0.28) recorded at these sites most likely represent the true seawater composition.

The differences in the bulk $^{187}Os/^{188}Os$ of age-equivalent samples (Fig. 3) among sections suggest that, unlike marine Sr isotope records, the utility of absolute $^{187}Os/^{188}Os$ values of marine records for stratigraphic correlation is limited. Nevertheless, the distinct features of the $^{187}Os/^{188}Os$ excursion that are correlatable among sections have significant potential as stratigraphic markers. This type of chemostratigraphy is analogous to determining ages by identifying oxygen isotope stages in marine records. Based on the records generated in this study and by [19], we recognize three such features of the $^{187}Os/^{188}Os$ excursion that can be used for stratigraphic correlation irrespective of the difference in absolute values of $^{187}Os/^{188}Os$ among sections (Figs. 2 and 3). These are (i) the initiation of $^{187}Os/^{188}Os$ decline, (ii) the Late Eocene $^{187}Os/^{188}Os$ minimum and (iii) the beginning of $^{187}Os/^{188}Os$ plateau following the rapid recovery from the $^{187}Os/^{188}Os$ minimum. Os isotope data from Site 1219, plotted on the depth scales of Site 1218 (Fig. 2) based on the precise lithostratigraphic correlation [21], show that the correlatable features of the $^{187}Os/^{188}Os$ excursion as mentioned above match within the depth of a meter or so between the sections analyzed from Sites 1218 and 1219, thus underscoring the chemostratigraphic importance of $^{187}Os/^{188}Os$ records generated in sections for which depth-correlation is established. The locations of these features in the studied sections are delineated below.

(i) The initiation of the $^{187}Os/^{188}Os$ decrease in the Late Eocene is observed at sites 1218 and 1219, and is captured within 1.5 m. The depth intervals capturing this decline are marked “1” in Fig. 2. Using the age model of [17], the timing of $^{187}Os/^{188}Os$ decline can be placed between 35.6 and 35.4 Ma in the record.

(ii) The Late Eocene $^{187}Os/^{188}Os$ minimum is best captured in records from ODP Sites 1218, 1219 and DSDP Site 522. Gaps in core recovery at DSDP site 574 makes it impossible to ascertain precisely the depth intervals capturing the Late Eocene $^{187}Os/^{188}Os$ minimum. The depth intervals capturing the $^{187}Os/^{188}Os$ minimum at Sites 1218, 1219 and 522 (interval “2” in Fig. 2) correspond between 34.4 and 34.6 Ma (the sample

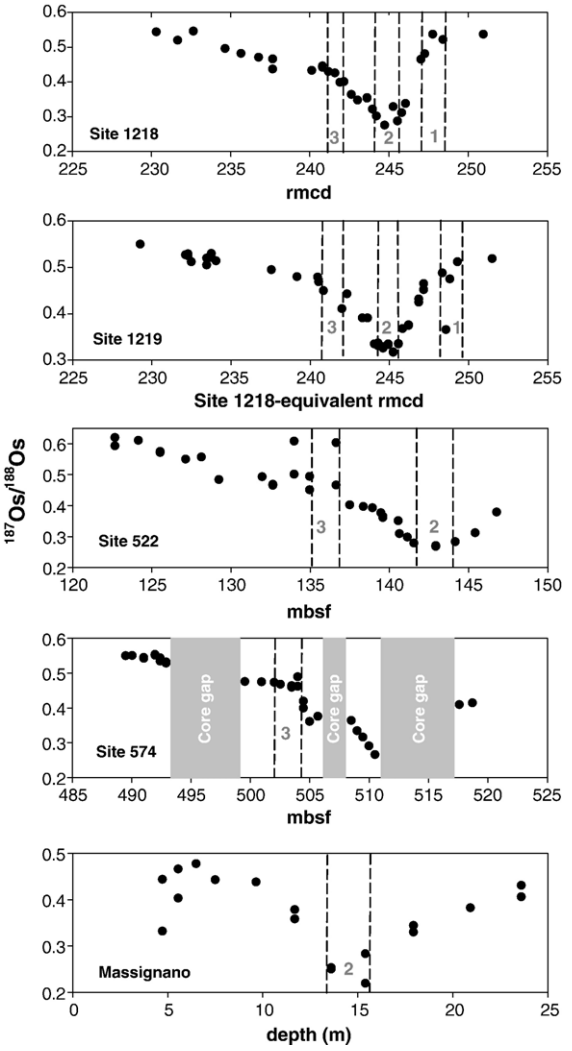

Fig. 2. Plot of bulk $^{187}Os/^{188}Os$ vs. sample depth for sections capturing the Eocene–Oligocene transition. $^{187}Os/^{188}Os$ data for the Site 1219 were plotted in the Site 1218-equivalent rmcd [21]. This plot reveals excellent match for the $^{187}Os/^{188}Os$ minimum and the features of the $^{187}Os/^{188}Os$ excursion between Sites 1218 and 1219. Data for DSDP Sites 522, 574 and Massignano are from [19]. In addition, unpublished $^{187}Os/^{188}Os$ data for Site 574 are also plotted. The intervals capturing the correlatable features of the Late Eocene $^{187}Os/^{188}Os$ excursion are shown by dashed vertical lines and marked as "1", "2" and "3".

depths of DSDP Site 522 have been translated to age based on the age model of [17].

(iii) A two-step rise of $^{187}Os/^{188}Os$ up to ~0.55 from the Late Eocene $^{187}Os/^{188}Os$ minimum is present in all the records except in the Massignano section. The first step involves the rapid recovery from the $^{187}Os/^{188}Os$ minimum to a plateau with $^{187}Os/^{188}Os$ values of ~0.43–0.45 at Site 1218, of ~0.47–0.48 at Site 1219, of 0.47–0.50 at Site 522 and of 0.46–0.49 at Site 574. The initiation of the $^{187}Os/^{188}Os$ plateau, also signifying the change in slope of the $^{187}Os/^{188}Os$ recovery (interval "3" in Fig. 2), falls between 33.7 and 33.9 Ma, very close to the initiation of the Oi-1 glaciation and EOB [17].

The beginning of the $^{187}Os/^{188}Os$ plateau (interval "3", Fig. 2) in the latest Eocene–earliest Oligocene can be used to track both the timing of the Oi-1 glaciation as well as the EOB in marine records, especially in pelagic clay sequences devoid of carbonates and well defined magnetic reversals. In addition, continuous and complete records of $^{187}Os/^{188}Os$ excursion at Sites 1218 and 1219 also provide a means of identifying hiatuses in sedimentation or refining age models at sites with incomplete core recovery across the EOT. For example, based on the age-$^{187}Os/^{188}Os$ plots for records from Sites 1218, 1219 and 522 (Fig. 3), the core gap at Site 574 immediately above the Oi-1 plateau (Fig. 2) can be placed between 32.8 and 33.1 Ma, whereas the core gap immediately below this section is between 33.9 and 34.2 Ma.

Based on the above discussion, we propose that the Late Eocene $^{187}Os/^{188}Os$ excursion provides three age control points (35.5 ± 0.1, 34.5 ± 0.1 and 33.8 ± 0.1 Myr). Given that slope of the age-$^{87}Sr/^{86}Sr$ curve across the EOT in the marine record is relatively less steep than later in the Cenozoic [30], it is likely that the marine $^{187}Os/^{188}Os$ records can provide more precise age-estimates relative to marine Sr isotope record in many instances. Whole ocean shifts in the $^{187}Os/^{188}Os$ during the glacial–interglacial climate cycles, on time scales of few tens of kilo years, are generally consistent among sections from sites that lie far apart from one another [31–34]. Therefore, high

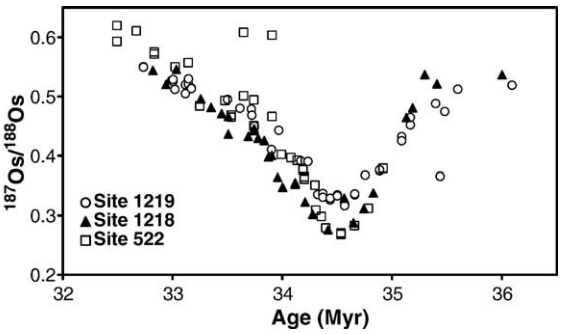

Fig. 3. Time profile of bulk $^{187}Os/^{188}Os$ at Sites 522, 1218 and 1219. Ages for sample depths were calculated based on age model of [17]. The Late Eocene $^{187}Os/^{188}Os$ minimum agrees well between Sites 1218 and 522, whereas $^{187}Os/^{188}Os$ values at Site 1219 are 5–10% higher relative to Site 1218 across the $^{187}Os/^{188}Os$ minimum.

resolution Os isotopic studies of sections with good age control during intervals of global events, when marine $^{187}Os/^{188}Os$ excursions are expected (e.g. Paleocene–Eocene thermal maximum, [18]), warrant detailed investigation. Such studies in cores with well defined age models, as available for Sites 1218 and 1219, can yield valuable chemostratigraphic markers and place useful constraints on interpretation of paleoclimatic records as discussed below.

4.2. $^{187}Os/^{188}Os$ of the sediment leachates: testing a hypothesis for the origin of the Late Eocene $^{187}Os/^{188}Os$ minimum

Ravizza and Peucker-Ehrenbrink [19] discounted the possibility of reduced continental Os flux as one of the causes of the Late Eocene $^{187}Os/^{188}Os$ minimum, as it required an unreasonably large decrease in the riverine Os flux. Instead, they inferred that increased unradiogenic Os flux to the oceans is the likely cause of this $^{187}Os/^{188}Os$ excursion. These authors considered two possible explanations for the Late Eocene $^{187}Os/^{188}Os$ minimum, (1) uplift and erosion of ultramafics associated with accretion of island arc terranes, and (2) increased contributions from extraterrestrial matter based on the observation of a protracted and higher IDP ^{3}He flux lasting about 2.5 Myr in the Late Eocene [8]. The lag (~1 Myr) between the IDP ^{3}He flux maximum and the $^{187}Os/^{188}Os$ minimum was attributed to the effects of Poynting–Robertson drag on extraterrestrial particles of different size.

In order to determine if the suggestion that an increase in cosmic dust flux was the cause for the Late Eocene $^{187}Os/^{188}Os$ minimum can be tested based on comparison of bulk-leachate $^{187}Os/^{188}Os$, we performed analysis of $^{187}Os/^{188}Os$ in sediment leachates. The motivation for this effort stems from the knowledge that analyses of leachates offer a means of identifying sediments in which $^{187}Os/^{188}Os$ of bulk sediments is significantly influenced by Os derived from nonhydrogenous sources, such as lithogenic material and/or particulate extraterrestrial material. Quantitative intepretations of bulk-leach differences in $^{187}Os/^{188}Os$ are based on isotope mass balance models that partition the total Os of bulk sediments into three isotopically distinct pools: lithogenic, extraterrestrial, and hydrogenous [32,35,36]. The isotopic composition of leachable Os is interpreted to closely represent the $^{187}Os/^{188}Os$ of the hydrogenous Os reservoir, and thus the $^{187}Os/^{188}Os$ of ancient seawater [26,37,38]. In the majority of studies used to reconstruct the marine Os isotope record, the total flux of Os to the sediment is dominated by hydrogenous Os so that differences between bulk sediment and leachate $^{187}Os/^{188}Os$ are indistinguishable [27,38]. In instances where $^{187}Os/^{188}Os$ of the bulk sediments and leachates differ significantly, this difference can reveal information about the various sources of dissolved and particulate Os contained in the sediment. For example, leachates of sediments collected from the basins receiving dominant dissolved Os contributions from ultramafics and arc-volcanics yielded lower $^{187}Os/^{188}Os$ relative to the bulk sediments [39] whereas the opposite is true if sediments contain significant extraterrestrial particulate Os [27,37,40]. Reported $^{187}Os/^{188}Os$ difference between dissolved and suspended/bed loads in rivers [41] also point to the utility of the leachate analysis. Hydrogen peroxide-sulfuric acid leaching has been used as a means of selectively dissolving the hydrogenous Os [26,37]. In this study, the sediments have been leached with 0.3 vol.% H_2O_2 in the presence of sulfuric acid for reasons described in the methods section earlier.

Analysis of leachates yields contrasting results between sites from the Atlantic and the Pacific (Fig. 4). At Sites 1218 and 1219, the $^{187}Os/^{188}Os$ values in the leachates are higher compared to the bulk composition of samples representing the intervals capturing the lowest $^{187}Os/^{188}Os$ in the excursion. This $^{187}Os/^{188}Os_{leachate} - ^{187}Os/^{188}Os_{bulk}$ difference is small before and after the Late Eocene excursion to low $^{187}Os/^{188}Os$. On the contrary, at Site 522 in the Atlantic, in records capturing the Late Eocene $^{187}Os/^{188}Os$

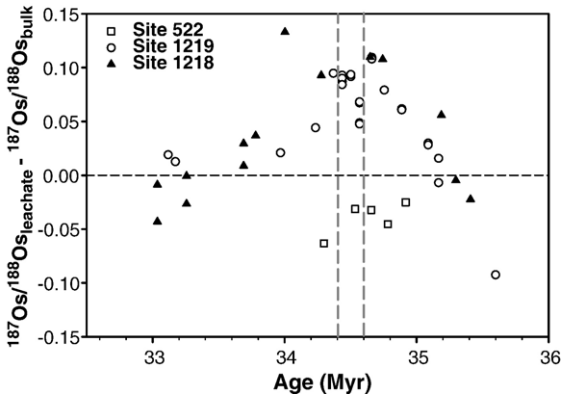

Fig. 4. Plot of difference in $^{187}Os/^{188}Os$ of leachates and bulk sediment vs. age of sample depth. Higher leachate-bulk difference for $^{187}Os/^{188}Os$ across the $^{187}Os/^{188}Os$ minimum is observed at Sites 1218 and 1219, whereas the opposite was observed at Site 522. Note that for some samples, available $^{187}Os/^{188}Os$ from replicate measurements of either bulk or leachate were used to calculate the leach-bulk difference. The vertical grey dashed lines represent the time intervals of the Late Eocene $^{187}Os/^{188}Os$ minimum (34.5 ± 0.1 Myr).

minimum, leachates yield lower values of $^{187}Os/^{188}Os$ relative to the bulk sediments. Whilst higher $^{187}Os/^{188}Os$ in the leachates, as observed for Leg 199 samples, support the presence of significant non-leachable particulate extraterrestrial Os component in the sediments deposited during this interval, observed lower $^{187}Os/^{188}Os$ in the leachates at Site 522 is not consistent with this interpretation. It is noteworthy that across the $^{187}Os/^{188}Os$ excursion, leachate $^{187}Os/^{188}Os$ observed at Sites 1218 and 1219 (0.37–0.40) are very different than that observed at Site 522 (0.24) and the agreement of $^{187}Os/^{188}Os$ among samples from Leg 199 Sites and Site 522 is better for the bulk analyses relative to the leachates. This suggests that $^{187}Os/^{188}Os$ of the leachates, for these samples, are most likely not representative of the seawater composition. Rather, as mentioned earlier, excellent match between $^{187}Os/^{188}Os$ records from Sites 522 and 1218 (Fig. 3) that are located in separate ocean basins widely apart from each other is an indication that the Late Eocene $^{187}Os/^{188}Os$ minima at these sites as measured in bulk sediments closely represent the seawater composition. One of the important features of leachate data of Leg 199 samples is variable and low proportions of leachable Os compared to the previous studies [26,31]. Across the $^{187}Os/^{188}Os$ minimum, only 1–3% of total Os is released during leaching whereas prior to the $^{187}Os/^{188}Os$ minimum in the Late Eocene, leachable Os accounts for as high as ~25% of total Os. Thus, possible impact of non-hydrogenous Os on the leachate $^{187}Os/^{188}Os$ will be enhanced in samples recording the $^{187}Os/^{188}Os$ minimum. We suggest a combination of the following could lead to the observed inconsistency in the leachate $^{187}Os/^{188}Os$ among sites from the Atlantic and the Pacific basins: leaching of labile terrigenous Os and/or diagenetically mobile Os, variable fractions of cosmic dust at different sites and incomplete recovery of hydrogenous Os. The results of leaching experiments in this study suggest that leachate $^{187}Os/^{188}Os$ of old radiolarian clay and nannofossil ooze samples as records of seawater composition should be interpreted with caution.

Enhanced cosmic dust flux in the Late Eocene as a cause for the Os isotope excursion in the Late Eocene [19] can not be ruled out. Although the results of the leaching experiments of our study are equivocal, consideration of some the following aspects suggests that it is not unreasonable to retain this hypothesis. First, contributions of Os to world oceans via eolian transport constitute an insignificant fraction of the amount of Os delivered by rivers [42]. Second, considering that the ultramafic rocks constitute volumetrically small proportion of the earth's surface today, it seems unlikely that this lithology was distributed widely enough to assume global significance. Third, it is already documented that there was an episode of enhanced cosmic dust flux in the Late Eocene [8]. In addition, data on abundance of terrigenous matter at Sites 1218 and 1219 [23] show that contributions from detrital particles do not exert noticeable influence on $^{187}Os/^{188}Os$ of sediments. This is illustrated in the plot of depth vs. the fractional abundance of terrigenous matter (Fig. 1). Interestingly, the Late Eocene $^{187}Os/^{188}Os$ minima at both sites roughly coincide with the corresponding local minima of terrigenous fractions. Furthermore, good match for $^{187}Os/^{188}Os$ records between Sites 1218 and 1219 in the Early Oligocene, when the abundances of terrigenous matter at Site 1219 were much higher relative to Site 1218, provide additional support to the notion that detrital particles are of negligible importance in regulating $^{187}Os/^{188}Os$ of sediments across the EOT.

It is important to note that unlike the transient $^{187}Os/^{188}Os$ excursion arising from the meteoritic impact across the Cretaceous–Tertiary boundary (<200 kyr, [20]), the Eocene–Oligocene $^{187}Os/^{188}Os$ excursion lasted for a duration of ~1.5 Myr. The gradual decline of $^{187}Os/^{188}Os$ in the Late Eocene, the long duration of the $^{187}Os/^{188}Os$ excursion and overall shape of Os isotope curve across the EOT cannot be attributed to a single extraterrestrial impact; they rather reflect a long term shift in the isotopic composition of Os delivered to the ocean via protracted higher cosmic dust flux [8]. Mass balance calculations, using a pre-excursion seawater $^{187}Os/^{188}Os$ value of 0.53 and the Late Eocene $^{187}Os/^{188}Os$ minimum value of 0.3 and assuming a simple two component mixing between seawater Os and extraterrestrial Os (with $^{187}Os/^{188}Os=0.13$), suggest that at the nadir of the $^{187}Os/^{188}Os$ excursion, Os contributions from cosmic dust fluxes were about ten fold higher compared to the modern value, a result similar to reported earlier [19].

It is observed that PGE concentration ratios (data to be reported elsewhere) do not become more chondritic across the $^{187}Os/^{188}Os$ minimum at Sites 1218 and 1219. Thus the PGE abundance patterns at these sites will seem inconsistent with enhanced contributions from cosmic dust in the Late Eocene if extraterrestrial PGE supplied to sediments had chondritic abundance pattern. One possible way to reconcile the non-chondritic character of the PGE abundance patterns with our interpretation of the Os isotope data is to invoke fractionation of PGE from one another due to ablation processes during atmospheric entry of extraterrestrial material. A recent study, based on fluxes of Ir and Pt in ice cores from Greenland, suggests that most of the

particulate flux of extraterrestrial material is vaporized during atmospheric entry and re-condensed into nanometer size particles [43]. Given the very refractory character of the PGE, substantial elemental fractionation between the vapor and the small amount of residual solid seems likely. For example, McNeil et al. [44] suggest that more volatile metals of the cosmic dust sublimates earlier and at higher altitude resulting in relative abundances of metals in the atmosphere that is disproportionate to abundances in meteoric material. Indeed, available data for Pt-rich nuggets of deep sea cosmic spherules show that fractionation of the PGE does occur [45]. Low Pd/Ir in the impact ejecta were explained by [46] in terms of PGE fractionation via loss of volatile PGE associated with atmospheric spherule condensation. More detailed knowledge of ablation of PGE from cosmic dust during atmospheric entry is required to rigorously assess whether this process can reconcile the observed PGE patterns across the Late Eocene Os isotope excursion with an increased flux of extraterrestrial material. Another scenario would be that PGE scavenged from seawaters overwhelm the signatures inherited from extraterrestrial particulates and/or that PGE of the cosmic particles are fractionated in the marine environment during their transport and deposition. Also, it is not known how the supply of PGE to the oceans via slow and prolonged delivery of extraterrestrial particles will influence the PGE abundances in marine sediments compared to the case of extraterrestrial impacts where the meteorites interact with the target rocks. Thus, models of physical mixing between extraterrestrial matter and sediments analogous to those applied to impact crater studies are likely inappropriate. A detailed discussion of the sources and processes regulating the PGE concentrations and patterns of the EOT sections at Sites 1218 and 1219 will be presented in a companion paper.

4.3. The Eocene–Oligocene $^{187}Os/^{188}Os$ excursion vis-à-vis Oi-1 glaciation

The records from sites 1218 and 1219 show that the rate of recovery from the Late Eocene $^{187}Os/^{188}Os$ minimum is roughly similar to the rate of decline in $^{187}Os/^{188}Os$ during the Late Eocene (Fig. 3). As discussed earlier, marine $^{187}Os/^{188}Os$ recovered and stabilized briefly forming a plateau during the Oi-1 glaciation, and then increased albeit with a shallower gradient to values (~0.54–0.55) that are higher compared to those at the initiation of the Late Eocene $^{187}Os/^{188}Os$ decline (~0.51–0.52). Such a two step rise of $^{187}Os/^{188}Os$ following the Late Eocene minimum is also apparent at DSDP Sites 522 and 574. Ravizza and Peucker-Ehrenbrink [19] observed that higher $^{187}Os/^{188}Os$ values following the $^{187}Os/^{188}Os$ excursion relative to those at the initiation of the excursion resulted in asymmetric shape of the E–O $^{187}Os/^{188}Os$ records, which was also observed in the low resolution E–O records of the North Pacific core LL44-GPC3 [26]. The complete Late Eocene $^{187}Os/^{188}Os$ excursions captured in individual sections from the ODP sites 1218 and 1219 show that the difference in $^{187}Os/^{188}Os$ between Late Eocene and Early Oligocene sections are relatively smaller, resulting in reduced asymmetry of the $^{187}Os/^{188}Os$ excursion compared to the results of [19]. The amplified asymmetry of the Late Eocene $^{187}Os/^{188}Os$ excursion observed in the study of [19] was presumably due to comparison between low $^{187}Os/^{188}Os$ in the Late Eocene observed at Massignano with much higher $^{187}Os/^{188}Os$ values during the Early Oligocene measured in sections from DSDP Sites 522 and 574.

The step-wise rise of marine $^{187}Os/^{188}Os$ following the Late Eocene $^{187}Os/^{188}Os$ minimum is noteworthy and is most likely related to effects of climate transition. Following the Late Eocene $^{187}Os/^{188}Os$ minimum, $^{187}Os/^{188}Os$ in sections from Sites 1218 and 1219 recover and stabilize briefly at values of ca. 0.43–0.45, which are significantly less compared to $^{187}Os/^{188}Os$ values at the initiation of the isotopic excursion (ca. 0.51–0.52, Figs. 2 and 3). These brief $^{187}Os/^{188}Os$ plateaus following the $^{187}Os/^{188}Os$ minimum coincide with the timing of rapid cooling and development of Oi-1 glaciation as shown in the plot of $^{187}Os/^{188}Os$ vs. benthic $\delta^{18}O$ at Sites 1218 and 522 (Fig. 5). In absence of additional perturbations other than the enhanced unradiogenic Os flux in the Late Eocene, marine $^{187}Os/^{188}Os$ in the Early Oligocene is expected to recover back to the pre-excursion values. Failure to do so is most likely a result of decrease in ^{187}Os flux to oceans driven by rapid cooling and aridity leading to the Oi-1 glaciation (at ca. 34 Myr). Rea and Lyle [5] suggested that increased burial of $CaCO_3$ in the deep ocean and drop of carbonate compensation depth by more than 1 km at the EOB requires rapid increase in the Ca inputs to the oceans by chemical weathering. The climate-induced perturbation of the marine Os isotope record across the EOB is difficult to resolve as it is superimposed upon the recovery from the Late Eocene $^{187}Os/^{188}Os$ minimum caused by contributions from cosmic dust.

Considering that bulk $\delta^{18}O$ values of benthic foraminifera reflect both temperature dependent isotope fractionation and changes in global ice volumes, it is desirable to deconvolute the effects of these two pro-

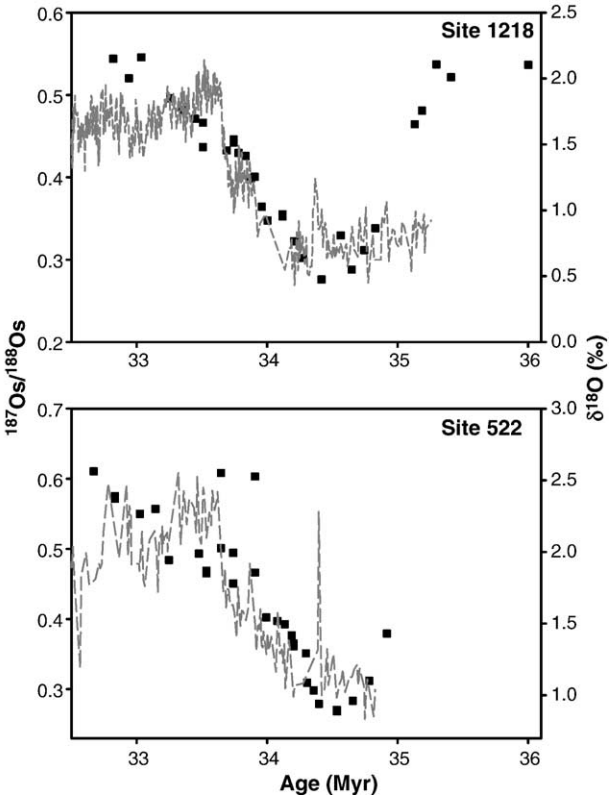

Fig. 5. Comparison of variations in bulk $^{187}Os/^{188}Os$ (filled squares) and benthic $\delta^{18}O$ (dashed lines) with time in sections from Sites 522 and 1218. At both sites a brief $^{187}Os/^{188}Os$ plateau following the $^{187}Os/^{188}Os$ minimum coincides with the rapid increase of benthic $\delta^{18}O$ during the development of the Oi-1 glaciation. Thereafter, $^{187}Os/^{188}Os$ rises when benthic $\delta^{18}O$ starts to decrease, signaling the decay of the Antarctic ice sheets ($\delta^{18}O$ data from [3,17]).

cesses in order to assess the role of change in ice volumes on continental weathering and thus on variations in marine $^{187}Os/^{188}Os$. In principle, Mg/Ca data can be used to calculate $\delta^{18}O$ of seawater ($\delta^{18}O_{sw}$) in the past [47,48], which is an indicator of variations in the ice volume. Lear et al. [47], based on Mg/Ca in benthic foraminifera, concluded that the Oi-1 glaciation was not accompanied by a decrease in deep-sea temperatures. Thus, $\delta^{18}O$ positive excursion of Oi-1 was mainly a result of increase in continental ice volume. Coxall et al. [17], however, observed that shift in $\delta^{18}O$ across the EOB at Site 1218 is too large to be explained by Antarctic ice-sheet growth alone and requires either global cooling and/or Northern Hemisphere glaciation. On the other hand, Lear et al. [48] observed an overall 2 °C increase in deep waters at Site 1218 associated with the Oi-1 glaciation. These authors also inferred a 2 °C cooling of intermediate waters at Site 522 during the first phase of $\delta^{18}O$ excursion associated with Oi-1, whereas apparent warming was observed both at Sites 522 and 1218 during the second phase. Comparison of the Mg/Ca data from Site 1218 with $^{187}Os/^{188}Os$ records across the EOT (Fig. 6) suggest that at Site 1218, deep water temperature dropped rapidly in the Late Eocene, coinciding with the decline of marine $^{187}Os/^{188}Os$. Existing data for Site 522 [19,47,48] do not show such a trend. Together, these lines of evidence suggest that meaningful comparison of variations in global ice volumes and marine $^{187}Os/^{188}Os$ awaits consistent reconstruction of global $\delta^{18}O_{sw}$. In the following we assess the influence of the Oi-1 glaciation on the marine Os isotope record based on $\delta^{18}O$ of benthic foraminifera.

Stabilization of $^{187}Os/^{188}Os$ during build-up of Oi-1 glaciation and rise of $^{187}Os/^{188}Os$ during the decay of the ice sheets is illustrated in the plot of $^{187}Os/^{188}Os$ vs. oxygen isotopic composition ($\delta^{18}O$) of benthic foraminifera at Sites 1218 and 522 (Fig. 5). The increase of $^{187}Os/^{188}Os$ coincides with the decrease of benthic $\delta^{18}O$ values, signaling deglacial melting. The observed trends between $^{187}Os/^{188}Os$ and $\delta^{18}O$ confirm our general understanding that the rate of release of ^{187}Os to oceans is accelerated during deglacial weathering either via preferential release of ^{187}Os from the freshly

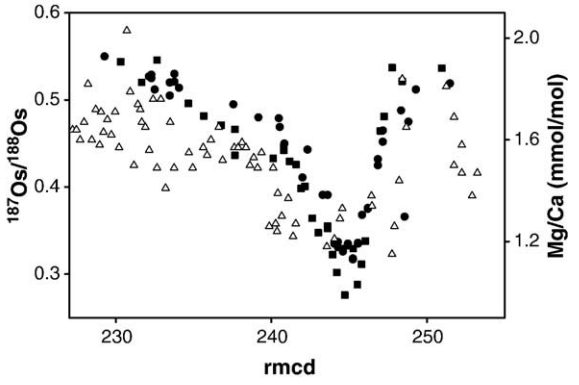

Fig. 6. Comparison of benthic Mg/Ca at Site 1218 (open triangles) with bulk $^{187}Os/^{188}Os$ at Site 1218 (filled squares) and Site 1219 (filled circles). Depth scale for the Site 1219 samples is in Site 1218-equivalent rmcd. Decline in $^{187}Os/^{188}Os$ during the Late Eocene is coeval with rapid decrease of Mg/Ca indicative of deep water cooling (Mg/Ca data from [48]).

exposed source rocks [49], or due to a higher continental dissolved Os flux due to enhanced weathering and water flux [32,34], or a combination of both. An increased rate of silicate weathering during deglaciation may have contributed to rapid drawdown of CO_2 from the atmosphere, thereby aiding in ice sheet stabilization [19]. While the hypothesis of 'deglacial weathering–CO_2 drawdown-ice sheet stabilization' in the Early Oligocene is yet to be tested, it draws support from the existing studies indicating that concentrations of atmospheric CO_2 dropped following the Oi-1 glaciation [50], and enhanced weathering fluxes of base cations and carbon on the continents immediately after the Oi-1 glaciation [14].

4.4. Extraterrestrial influence on climate change across the Eocene–Oligocene transition

The paleoclimatic significance of the Late Eocene excursion to low $^{187}Os/^{188}Os$ ratios remains uncertain. The most recent discussion of the potential paleoclimatic significance of the Late Eocene Os isotope excursion [19] pointed out that the nadir of the excursion preceded the Oi-1 glaciation and thus might be causally linked to this important paleoclimate event. However, this discussion offers no specific mechanism by which an episode of increased cosmic dust flux might influence climate. In light of subsequent studies that emphasize the abrupt nature of the Oi-1 glaciation and its significance as a major Cenozoic climate transition driven by CO_2 draw-down below a critical "threshold" level [11,17], we present a speculative hypothesis that links increased flux of particulate extraterrestrial material to CO_2 draw-down.

We suggest that an episode of increased delivery of extraterrestrial particles to the Earth, lasting for 2.5 Myr [8], has the potential to perturb long-term patterns of organic and inorganic carbon burial by substantially enhancing the flux of biologically important trace metals to the surface ocean and thus triggering high surface productivity. It is widely recognized that productivity in large parts of the modern open ocean is limited by the availability of Fe [51,52]. Other biologically essential trace metals, such as Zn and Co may also be important in regulating the relative amounts of biogenic carbonate and organic carbon production ([53] and references therein). Existing studies point to higher productivity in many parts of the oceans in the Late Eocene. It has been suggested that some part of the equatorial Atlantic experienced enhanced productivity and carbon burial in the Late Eocene [54]. Schumacher and Lazarus [55] show that the productivity in the Southern Ocean started increasing in the Late Eocene and continued through the EOT, whereas in the equatorial oceans no clear trend was apparent. Paleobotanical studies on fossil floras from Germany suggest that atmospheric CO_2 concentration decreased after Late Eocene and continued to decrease until Early Oligocene [56]. Isotopic measurements of alkenones suggest atmospheric CO_2 concentrations started declining rapidly following the EOB [50]. On the other hand, Sarkar et al. [15] inferred that atmospheric CO_2 concentration dropped dramatically across the EOB and attributed the CO_2 drop across the EOT to enhanced silicate weathering and carbon burial via Himalayan uplift. Trace metal fertilization of the surface ocean by extraterrestrial particles represents a viable alternative mechanism for CO_2 drawdown prior to the Oi-1 glaciation. Available data on eolian flux to the Pacific throughout the Cenozoic indicate that warm humid Eocene conditions were associated with low eolian flux to the Pacific compared to modern conditions [57]. Calculations suggest that today interplanetary dust particles may play an important control on carbon cycling in the modern ocean by supplying significant amount of bioavailable Fe; up to 300% of eolian Fe flux and 20% of the upwelling Fe flux to the Southern Ocean [58]. Thus, the approximately ten fold increase in Late Eocene extraterrestrial Fe flux relative to modern condition (similar to Os flux) may well have had a significant impact on marine productivity and carbon export, especially in regions where Fe and trace metal deficiency hindered primary productivity.

Recently Coxall et al. [17] postulated that a specific configuration of Earth's orbit, one favoring colder summers, was the ultimate trigger for the Oi-1 event.

These authors, however, recognized that similar orbital conditions recurred approximately every 1.2 Myr (the obliquity minimum) and 2.4 Myr (the eccentricity minimum) during the past 40 Myr, and emphasized the importance of some other conditioning factor (e.g. long term decline in atmospheric CO_2 levels). It is possible that ocean fertilization driven by the Late Eocene meteoric shower in the million years prior to the Oi-1 event may have caused CO_2 draw-down, establishing the low CO_2 conditions required for orbital changes to trigger the Oi-1 glaciation. Based on the observations of increasing productivity in the Late Eocene and the earliest Oligocene, and that the positive $\delta^{13}C$ excursion during Oi-1 lags (by ca. 20 kyr) the $\delta^{18}O$ maximum, Diester-Haass and Zahn [59] suggested that increased marine productivity and organic carbon burial in the high to mid and low southern latitudes may have contributed to the earliest Oligocene climate transition. Increase in $\delta^{13}C$ of benthic foraminifera in the Late Eocene is more common in the southern latitude. For example, a tend of increasing benthic $\delta^{13}C$ in the Late Eocene is observed at Site 522 in the Atlantic [3] whereas at Site 1218 in the Pacific, benthic $\delta^{13}C$ was observed to increase across the Eocene–Oligocene transition with no clear trend in its variation in the Late Eocene [17].

Reported records of higher and variable pCO_2 levels in the Late Eocene [50] are difficult to correlate with the $^{187}Os/^{188}Os$ records of this study, however, the hypothesis proposed above draws support from the studies suggestive of cooling and existing glacial condition prior to the Oi-1 glaciation. Data on nannofossil assemblages from sections in the Southern Ocean show that there were several minor cooling events from 36 Ma to 34 Ma [60]. Based on analysis of quartz grain microtextures, Strand et al. [61] inferred that glacial conditions were established in the Antarctica by the Upper Eocene.

5. Conclusions

1. This study corroborates that the Late Eocene $^{187}Os/^{188}Os$ minimum is characteristic of the global oceans and suggests that the $^{187}Os/^{188}Os$ excursion can be placed at 34.5 ± 0.1 Ma in the marine records.
2. Three distinct and correlatable features of the Late Eocene $^{187}Os/^{188}Os$ excursion are proposed to serve as chemostratigraphic markers that provide age control points with a precision of the order of ± 0.1 Myr. These features have great stratigraphic potential in sections devoid of carbonates and well defined magnetic reversals.
3. Combined leachate and bulk $^{187}Os/^{188}Os$ data across the Late Eocene $^{187}Os/^{188}Os$ excursion for the records from the Pacific and the Atlantic suggest that leachate $^{187}Os/^{188}Os$ obtained in this study do not represent the seawater composition and can not be used to identify an episode of increased cosmic dust flux.
4. Comparison of marine $^{187}Os/^{188}Os$ and $\delta^{18}O$ records provide important new data on climate-weathering feedbacks. Results from this study suggest that during the time of rapid cooling and build-up of ice during Oi-1, weathering fluxes to oceans decreased. Following this, increase of marine $^{187}Os/^{188}Os$ coincided with the initiation of Oi-1 termination (lowering of benthic $\delta^{18}O$), suggestive of higher ^{187}Os flux to the oceans via enhanced deglacial weathering and/or preferential release of ^{187}Os. This behavior is consistent with higher weathering fluxes of base cations and carbon following the Oi-1 glaciation and supports the hypothesis that deglaciation is associated with accelerated rates of chemical weathering.
5. We hypothesize that enhanced supply of trace elements from higher cosmic dust flux in the Late Eocene may have caused a surge in the ocean productivity and enhanced burial of organic carbon, thus contributing to rapid cooling and Oi-1 glaciation. This hypothesis draws support from circumstantial evidences of Late Eocene cooling and high productivity in the Southern Ocean.

Acknowledgements

We are thankful to H. Pälike, P. A. Wilson, M. Lyle, C. H. Lear, H. K. Coxall and M. D. Vanden Berg for generously providing data on Leg 199 cores. We are especially indebted to H Pälike for sharing the pre-publication data of his age model. Two anonymous reviewers are thanked for their constructive comments on the manuscript. We thank Tracy Atwood and Dave Schneider in the WHOI ICP Facility for help with some preliminary Os isotope analyses. The samples analyzed in this study were provided by the Ocean Drilling Program. This study was supported by NSF awards OCE-0118380, EAR-0215297 and EAR-0215297. This is SOEST contribution number 6653.

References

[1] J.P. Kennett, N.J. Shackleton, Oxygen isotopic evidence for the development of the psychrosphere 38 Myr ago, Nature 260 (1976) 513–515.

[2] K.G. Miller, J.D. Wright, R.G. Fairbanks, Unlocking the ice house: Oligocene–Miocene oxygen isotopes, eustasy and margin erosion, J. Geophys. Res. 96 (1991) 6829–6848.
[3] J.C. Zachos, T.M. Quinn, K.A. Salamy, High-resolution (10^4 years) deep-sea foraminiferal stable isotope records of the Eocene–Oligocene climate transition, Paleoceanography 11 (1996) 251–266.
[4] T.H. van Andel, Mesozoic/Cenozoic calcite compensation depth and the global distribution of calcareous sediments, Earth Planet. Sci. Lett. 26 (1975) 187–194.
[5] D.K. Rea, M.W. Lyle, Paleogene calcite compensation depth in the eastern subtropical Pacific: answers and questions, Paleoceanography 20 (2005) PA 1012. doi:10.1029/2004PA001064.
[6] C. Koeberl, C.W. Poag, W.U. Reimold, D. Brandt, Impact origin of the Chesapeake Bay structure and the source of the North American tektites, Science 271 (1996) 1263–1266.
[7] R. Bottomley, R. Grieve, D. York, V.L. Masaitis, The age of the Popigai impact events and its relation to events at the Eocene/Oligocene boundary, Nature 388 (1997) 365–368.
[8] K.A. Farley, A. Montanari, E.M. Shoemaker, C.S. Shoemaker, Geochemical evidence for a comet shower in the Late Eocene, Science 280 (1998) 1250–1253.
[9] J.P. Kennett, Cenozoic evolution of Antarctic glaciation, the circum-Antarctic ocean, and their impact on global paleoceanography, J. Geophys. Res. 82 (1977) 3843–3860.
[10] C.E. Stickley, H. Brinkhuis, S.A. Schellenberg, A. Sluijs, U. Rohl, M. Fuller, M. Grauert, M. Huber, J. Warnaar, G.L. Williams, Timing of the nature of the deepening of the Tasmanian Gateway, Paleoceanography 19 (2004) A4027. doi:10.1029/2004PA001022.
[11] R.M. DeConto, D. Pollard, Rapid Cenozoic glaciation of Antarctica induced by declining atmospheric CO_2, Nature 421 (2003) 245–249.
[12] P. Fawcett, M.B.E. Boslough, Climatic effects of an impact-induced equatorial debris ring, J. Geophys. Res. 107 (2002). doi:10.1029/2001JD001230.
[13] H.B. Vonhof, J. Smit, H. Brinkhuis, A. Motanari, A.J. Nederbragt, Global cooling accelerated by early late Eocene impacts?, Geology 28 (2002) 687–690.
[14] E.A. Bestland, Weathering flux and CO_2 consumption determined from paleosol sequences across the Eocene–Oligocene transition, Paleogeogr. Paleoclimatol. Paleoecol. 156 (2000) 301–326.
[15] A. Sarkar, S. Sarangi, S.K. Bhattacharya, A.K. Ray, Carbon isotopes across the Eocene–Oligocene boundary sequence of Kutch, western India: implications to oceanic productivity and pCO_2 change, Geophys. Res. Lett. 30 (2003) 2003. doi:10.1029/2002GL016541.
[16] G.J. Retallack, Cenozoic expansion of grasslands and climate cooling, J. Geol. 109 (2001) 407–426.
[17] H.K. Coxall, P.A. Wilson, H. Pälike, C.H. Lear, J. Backman, Rapid stepwise onset of Antarctic glaciation and deeper calcite compensation in the Pacific Ocean, Nature 433 (2005) 53–57.
[18] G. Ravizza, R.N. Norris, J. Blusztajn, An osmium isotope excursion associated with the late Paleocene thermal maximum: evidence of intensified chemical weathering, Paleoceanography 16 (2001) 155–163.
[19] G. Ravizza, B. Peucker-Ehrenbrink, The marine $^{187}Os/^{188}Os$ record of the Eocene–Oligocene transitions: the interplay of weathering and glaciation, Earth Planet. Sci. Lett. 210 (2003) 151–165.
[20] G. Ravizza, B. Peucker-Ehrenbrink, Chemostratigraphic evidence of Deccan Volcanism from the marine osmium isotope record, Science 302 (2003) 1392–1395.
[21] H. Pälike, T. Moore, J. Backman, I. Rafii, L. Lanci, J.M. Parés, T. Janecek, Integrated stratigraphic correlation and improved composite depth scales for ODP Sites 1218 and 1219. In: Wilson, P.A., Lyle, M., and Firth, J.V. (Eds.), Proc. ODP, Sci. Results, 199 [Online], http://www-odp.tamu.edu/publications/199_SR/213/213.htm.
[22] M. Lyle, P.A. Wilson, T.R. Janecek, et al., in: Proceedings of the Ocean Drilling Program, Initial Reports, vol. 199 (online), Ocean Drilling Program, College Station, Texas, 2002, http://www-odp.tamu.edu/publications/199_IR/199ir.htm.
[23] M.D. Vanden Berg, R.D. Jarrard, Cenozoic mass accumulation rates in the equatorial Pacific based on high-resolution mineralogy of Ocean Drilling Program Leg 199, Paleooceanography 19 (2004). doi:10.1029/2003PA000298.
[24] G. Ravizza, D. Pyle, PGE and Os isotopic analyses of single sample aliquots with NiS fire assay preconcentration, Chem. Geol. 141 (1997) 251–268.
[25] D.R. Hassler, B. Peucker-Ehrenbrink, G.E. Ravizza, Rapid determination of Os isotopic composition by sparging OsO_4 into a magnetic-sector ICP-MS, Chem. Geol. 166 (2000) 1–14.
[26] W.J. Pegram, K.K. Turekian, The osmium isotopic composition change of Cenozoic sea water as inferred from a deep-sea core corrected for meteoritic contributions, Geochim. Cosmochim. Acta 63 (1999) 4053–4058.
[27] B. Peucker-Ehrenbrink, G. Ravizza, A.W. Hofmann, The marine $^{187}Os/^{186}Os$ record of the past 80 million years, Earth Planet. Sci. Lett. 130 (1995) 155–167.
[28] K.K. Turekian, W.J. Pegram, Os isotope record in a Cenozoic deep-sea core: its relation to global tectonics and climate, in: W.F. Ruddiman (Ed.), Tectonic Uplift and Climate Change, Plenum Press, New York, 1997, pp. 383–397.
[29] K.W. Burton, B. Bourdon, J.-L. Birck, C.J. Allegre, J.R. Hein, Osmium isotope variations in the oceans recorded by Fe–Mn crusts, Earth Planet. Sci. Lett. 171 (1999) 185–197.
[30] J.M. McArthur, R.J. Howarth, T.R. Bailey, Strontium isotope stratigraphy: LOWESS Version 3: best fir to the marine Sr-isotope curve for 0–509 Ma and accompanying look-up table for deriving numerical age, J. Geol. 109 (2001) 155–170.
[31] R. Oxburgh, Variations in the osmium isotope composition of sea water over the past 200,000 years, Earth Planet. Sci. Lett. 159 (1998) 183–191.
[32] B. Peucker-Ehrenbrink, G. Ravizza, The marine osmium isotope record, Terra Nova 2 (2000) 205–219.
[33] G.A. Williams, K.K. Turekian, The glacial–interglacial variation of seawater osmium isotopes as recorded in Santa Barbara Basin, Earth Planet. Sci. Lett. 228 (2004) 379–389.
[34] T.K. Dalai, K. Suzuki, M. Minagawa, Y. Nozaki, Variations in seawater osmium isotope composition since the last glacial maximum: A case study from the Japan Sea, Chem. Geol. 220 (2005) 303–314.
[35] B.K. Esser, K.K. Turekian, The accretion rate of extraterrestrial particles determined from osmium isotope systematics of Pacific pelagic clay and manganese nodules, Geochim. Cosmochim. Acta 52 (1988) 1383–1388.
[36] B. Peucker-Ehrenbrink, Accretion rate of extraterrestrial matter during the last 80 million years and its effect on the marine osmium isotope record, Geochim. Cosmochim. Acta 60 (1996) 3187–3196.

[37] W.J. Pegram, S. Krishnaswami, G.E. Ravizza, K.K. Turekian, Record of seawater $^{187}Os/^{186}Os$ variation through the Cenozoic, Earth Planet. Sci. Lett. 113 (1992) 569–576.
[38] D.N. Reusch, G. Ravizza, K.A. Maasch, J.D. Wright, Miocene seawater $^{187}Os/^{188}Os$ ratios inferred from metalliferous carbonates, Earth Planet. Sci. Lett. 160 (1998) 163–178.
[39] C.E. Martin, B. Peucker-Ehrenbrink, G.J. Brunskill, R. Szymczak, Sources and sinks of unradiogenic osmium runoff from Papua New Guinea, Earth Planet. Sci. Lett. 183 (2000) 261–264.
[40] W.J. Pegram, B.K. Esser, S. Krishnaswami, K.K. Turekian, The isotopic composition of the leachable osmium from river sediments, Earth Planet. Sci. Lett 128 (1994) 591–599.
[41] Y. Huh, J.-L. Birck, C.J. Allegre, Osmium isotope geochemistry in the Mackenzie River Basin, Earth Planet. Sci. Lett. 222 (2004) 115–129.
[42] G.A. Williams, K.K. Turekian, Atmospheric supply of osmium to the oceans, Geochim. Cosmochim. Acta 66 (2002) 3789–3791.
[43] P. Gabrielli, C. Barbante, J.M.C. Plane, A. Varga, S. Hong, G. Cozzi, V. Gaspari, F.A.M. Planchon, W. Cairns, C. Ferrari, P. Crutzen, P. Cescon, C.F. Bourtron, Meteoric smoke fallout over the Holocene epoch revealed by iridium and platinum in Greenland ice, Nature 432 (2004) 1011–1014.
[44] W.J. McNeil, S.T. Lai, E. Murad, Differential ablation of cosmic dust and implications for the relative abundances of atmospheric metals, J. Geophys. Res. 103 (1998) 10899–10911.
[45] Ph. Bonté, C. Jéhanno, M. Mauratte, D.E. Brownlee, Platinum metals and microstructure in magnetic deep sea cosmic spherules, Proc. seventeenth lunar and planetary science conference Part 2, J. Geophys. Res. 92 (1987) E641–E648.
[46] A. Glikson, C. Allen, Iridium anomalies and fractionated siderophile element patterns in impact ejecta, Brockman Iron Formation, Hamersley Basin, Western Australia: evidence for a major asteroid impact in simatic crustal regions of the early Proterozoic earth, Earth Planet. Sci. Lett. 220 (2004) 247–264.
[47] C.H. Lear, H. Elderfield, P.A. Wilson, Cenozoic deep-sea temperatures and global ice volumes from Mg/Ca in benthic foraminiferal calcite, Science 287 (2000) 269–272.
[48] C.H. Lear, Y. Rosenthal, H.K. Coxall, P.A. Wilson, Late Eocene to early Miocene ice sheet dynamics and the global carbon cycle, Paleoceanography 19 (2004) A4015. doi:10.1029/2004PA001039.
[49] B. Peucker-Ehrenbrink, J.D. Blum, The effects of global glaciation on the osmium isotopic composition of continental runoff and seawater, Geochim. Cosmochim. Acta 62 (1998) 3193–3203.
[50] M. Pagani, J. Zachos, K.H. Freeman, B. Tipple, S. Bohaty, Marked decline in atmospheric carbon dioxide concentrations during the Paleogene, Science 309 (2005) 600–603.
[51] J.H. Martin, S.E. Fitzwater, R.M. Gordon, Iron deficiency limits phytoplankton growth in Atlantic waters, Glob. Biogeochem. Cycles 4 (1990) 5–12.
[52] F.M.M. Morel, R.J.M. Hudson, N.M. Price, Limitation of productivity by trace metals in the sea, Limnol. Oceanogr. 36 (1991) 1742–1755.
[53] K.G. Schulz, I. Zondervan, L.J.A. Gerringa, K.R. Timmermans, M.J.W. Veldhuis, U. Riebessel, Effect of trace metal availability on cocolithophorid calcification, Nature 430 (2004) 673–676.
[54] T. Wagner, Late Cretaceous to early Quaternary organic sedimentation in the eastern Equatorial Atlantic, Paleogeogr. Paleoclimatol. Paleoecol. 179 (2002) 113–147.
[55] S. Schumacher, D. Lazarus, Regional differences in pelagic productivity in the late Eocene to early Oligocene—a comparison of southern high latitudes and lower latitudes, Paleogeogr. Paleoclimatol. Paleoecol. 214 (2004) 243–263.
[56] A. Roth-Nebelsick, T. Utescher, V. Mosbrugger, L. Diester-Haass, H. Walther, Changes in atmospheric CO_2 concentrations and climate from the Late Eocene to Early Miocene: paleobotanical reconstruction based on fossil floras from Saxony, Germany, Paleogeogr. Paleoclimatol. Paleoecol. 205 (2004) 43–67.
[57] D.K. Rea, Changes in atmospheric circulation during the latest Paleocene and earliest Eocene epochs and some implications for the global climate regime, in: M.-P. Aubry, S. Lucas, W.A. Berggren (Eds.), Late Paleocene–Early Eocene climatic and biotic events in the marine and terrestrial records, Columbia University Press, New York, 1998, pp. 118–123.
[58] K.S. Johnson, Iron supply and demand in the upper ocean: is extraterrestrial dust a significant source of bioavailable iron?, Glob. Biogeochem. Cycles 15 (2001) 61–63.
[59] L. Diester-Haass, R. Zahn, Paleoproductivity increase at the Eocene–Oligocene climatic transition: ODP/DSDP sites 763 and 592, Paleogeogr. Paleoclimatol. Paleoecol. 172 (2001) 153–170.
[60] D. Persico, G. Villa, Eocene–Oligocene calcareous nannofossils from Maud Rise and Kerguelen Plateau (Antarctica): paleoecological and paleoceanographic implications, Mar. Micropaleontol. 52 (2004) 153–179.
[61] K. Strand, S. Passchier, J. Näsi, Implications of quartz grain microtextures for onset Eocene/Oligocene Glaciation in Prydz Bay, ODP Site 1166, Antarctica, Paleogeogr. Paleoclimatol. Paleoecol. 198 (2003) 101–111.